The dynamic characteristics of a diamagnetic levitated electrostatic motor

Yuanping XU [a], Yang WANG [a], Jarir MAHFOUD [b], Riwang LING [a], Jin ZHOU [a]
a Nanjing University of Aeronautics and Astronautics, Yudao Street, Nanjing, China, ypxu@nuaa.edu.cn
b University of Lyon, Lyon, France

Abstract

Diamagnetic Levitation emerges as a promising approach to tackle this friction issue. Due to the challenges of friction in micro motors, diamagnetic levitation emerges as a promising approach to tackle this friction issue and is essential in further developing high-speed, low-energy micro motors. Diamagnetic Levitated Electrostatic Motor has huge potential for development with the advantage of frictionless and passively stable levitation. This paper focuses on the model of the dynamics parameters of diamagnetical levitated rotor in order to accurately calculate the dynamic response of the rotor, which is important for optimising the performance of diamagnetical levitated electrostatic motor.

Therefore, this paper first establishes the kinetic equations of a diamagnetic levitated electrostatic motor and proposes a method for correcting and identifying the magnetic field parameters of permanent magnets based on the equivalent current model. Then, the diamagnetic force on the suspended rotor is modeled, which leads to the investigation of the distribution of the equivalent stiffness in the rotor dynamics system. The electromagnetic forces that impede the motion of the levitated rotor are then modeled based on the principle of electromagnetic induction, thus exploring the distribution characteristics of the damping parameters in the kinematic equations. At last, The radial vibration characteristics of the levitated rotor during operation are investigated by means of numerical simulations, and relevant experiments are designed to verify them.

Keywords: *Diamagnetic Levitation, Electrostatic Motor, Modeling.*

1. Introduction

With the development of MEMS technology, micro motors are the core parts of MEMs for realizing energy conversion, function-driven, and precision control, performing the combined functions of precision actuation and control in critical areas such as aerospace, micro-robotics, and biomedicine.

Diamagnetic levitation refers to the free levitation of diamagnetic object in magnetic field, which is not limited by Earnshaws' theorem[1], to achieve a constant, passive levitation of the diamagnetic object at room temperature without the need for an energy supply. With the inherent merits of frictionless, passive self-stabilization, and increased buoyancy-weight ratio, diamagnetic levitation emerges as a promising application in the micromotor.With the development of drive technology for diamagnetic levitated motors, the miniaturization and increase in speed of diamagnetic levitated motors have been accompanied by the problem of their severe vibration at high-speed operation, which limits further optimization of the performance of diamagnetic levitated electrostatic motors.

This paper investigates the force characteristics of the diamagnetic rotor. It completes modeling dynamic parameters of the diamagnetic rotor and predicting the vibrations in the magnetic levitated electrostatic motor's open-loop rotation.

The first section describes the operating principle of the diamagnetic levitated electrostatic motor and the kinematic characteristics of the levitated rotor. Then the second section develops mathematical models for correcting and identifying magnetic field parameters, diamagnetic forces, and electromagnetic damping forces. Then the third section corresponding experiments are designed to validate the above proposed mathematical model and analyze the dynamic response characteristics of the levitated rotor during the operation of the diamagnetic levitated electrostatic motor. The fourth section concludes with a full summary.

2. Diamagnetic levitated electromagnetic motor

Fig.1 shows a schematic diagram of the stable levitation of the pyrolytic graphite disc. The "concave" magnetic field generated by the permanent toroidal magnets forms a potential trap structure in the horizontal plane, with the minimum value point on the central axis. The magnetic field structure can generate a radial diamagnetic force against the levitated rotor toward the minimum value point. Meanwhile, the "convex" magnetic field generated by the cylindrical permanent magnets gives the levitated rotor a significant magnetic potential energy, which forms a clear potential energy trap

structure in the axial direction with the gravitational potential energy. The potential energy trap in the axial direction can generate an axial antimagnetic force against a suspended rotor pointing at a minimum value point. The levitated rotor achieves stable levitation at the intersection of the axial and radial directions.

Fig.2 shows a schematic diagram of the diamagnetic levitated electromagnetic motor, which combines diamagnetic levitated technology with electrostatic drives, using glass as the dielectric rotor[2-3]. The levitated rotor is constituted of a pyrolytic graphite disc (φ10×0.5mm) and a glass disc (φ10×0.15mm), as shown in Figure 2. For the PM array, a concentric ring-shaped magnet (φ18.68×φ7.96×12mm) encircling a cylinder magnet (φ7.94×12mm) with an opposite axial magnetization pattern that provides the radial forces; when the stator is supplied with three-phase AC high voltages, a rotating electric field above the stator will be generated which causes a lateral driven force that propels the glass disc to move based on the dielectric relaxation.

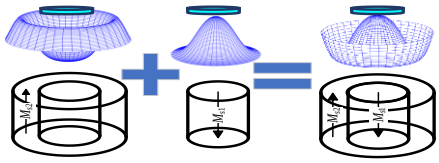

Fig.1 Diamagnetic levitation of the rotor

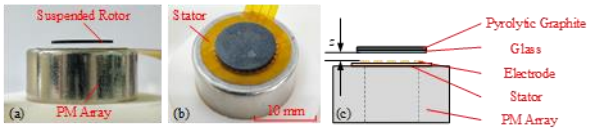

Fig.2 Diamagnetic levitated electromagnetic motor

3. Modelling and calculation of dynamics equation

3.1 Diamagnetic Force

First, the equivalent current model is used to analyze the PM (permanent magnets)[4]. According to this model, under ideal homogeneous magnetization conditions, the magnetic effects of the nuclear currents within the permanent magnet cancel each other out and appear as surface currents on a macroscopic scale. The permanent magnet with a uniform magnetization distribution can be equated to a surface current source distributed on the boundary surface of the magnetizing distribution region.In the column coordinate system, the magnetic flux density generated by a cylindrical permanent magnet at any point in space can be expressed as,

$$\boldsymbol{J}_{\boldsymbol{M}} = \boldsymbol{M} \times \boldsymbol{e}_{\boldsymbol{n}} = M_s \sin\theta \cdot \boldsymbol{e}_{\boldsymbol{\phi}} \tag{1}$$

$$\boldsymbol{B} = \frac{\mu_0}{4\pi} \oiint_S \frac{\boldsymbol{J}_M \times \boldsymbol{e}_R}{|P - P'|^2} ds = \frac{\mu_0}{4\pi} \oiint_S \frac{M_s \cdot \boldsymbol{e}_\phi \times \boldsymbol{e}_R}{|\boldsymbol{P} - \boldsymbol{P}'|^2} \sin\theta ds \tag{2}$$

where $\boldsymbol{J_M}$ is the equivalent surface current density, $\boldsymbol{M_s}$ stands for the magnetization,θ represents the angle between the direction of magnetization and the normal vector of the equivalent current surface, μ0 is the magnetic permeability of vacuum, P is the source point, P' is the observation point.

The disconnected end face of the permanent magnet causes its magnetization to be in an open circuit, suffering from a demagnetization field[5]. This effect results in an inconsistent magnetic field inside the permanent magnet and does not allow for absolutely uniform magnetization of the permanent magnet. Moreover, according to theoretical proof, only permanent ellipsoidal magnets can meet the requirements for uniform magnetization. The variable magnetization inside the miniature permanent magnets leads to a considerable deviation from the ideal distribution of the external magnetic field, significantly affecting the diamagnetic force calculation. As shown in Figure 3, according to the experiment of magnetic field measurements, this paper equates the magnetized region at the end of the columnar permanent magnet to an ellipsoidal homogeneously magnetized area.

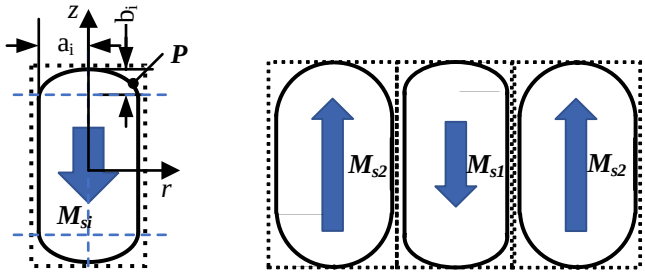

(a) Cylindrical permanent magnet (b) permanent magnets array

Fig.3 Magnetization distribution of PM array

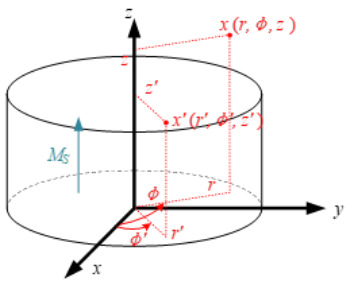

Fig.4 PM Columnar Coordinate System

Based on (2), the equivalent current model for columnar permanent magnets can be obtained as follows

$$\boldsymbol{B} = \frac{\mu_0 M_s}{4\pi} \int_{z1}^{z2} \int_0^{2\pi} \frac{\boldsymbol{e}_{\phi'} \times \boldsymbol{e}_R}{|\boldsymbol{P} - \boldsymbol{P}'|^2} r'(z') d\theta' dz' = \frac{\mu_0 M_s}{4\pi} \oiint_{S_1} \frac{\boldsymbol{e}_{\phi'} \times \boldsymbol{e}_R}{|\boldsymbol{P}_1 - \boldsymbol{P}'|^2} \frac{R(z')}{R'} \frac{|\boldsymbol{P}_1 - \boldsymbol{P}'|^2}{|\boldsymbol{P} - \boldsymbol{P}'|^2} ds' \tag{3}$$

where S_1 is the boundary surface of the magnetizing distribution region, R' is maximum radius of cross-section, $R(z')$ is radius of the cross-section with z-axis coordinate z'. Based on (5), a new equivalent current model can be obtained as fellows

$$\boldsymbol{J}_{M1}(z') = \frac{R(z')}{R'} \frac{|\boldsymbol{P}_1 - \boldsymbol{P}'|^2}{|\boldsymbol{P} - \boldsymbol{P}'|^2} \tag{4}$$

$$\boldsymbol{B} = \frac{\mu_0}{4\pi} \oiint_{S_1} \frac{\boldsymbol{J}_{M1}(z') \times \boldsymbol{e}_R}{|\boldsymbol{P}_1 - \boldsymbol{P}'|^2} ds' \tag{5}$$

where $\boldsymbol{J_{M1}}$ is the equivalent surface current density. Based on the above model, the equivalent surface current distribution of the permanent magnets is shown in Figure 5.

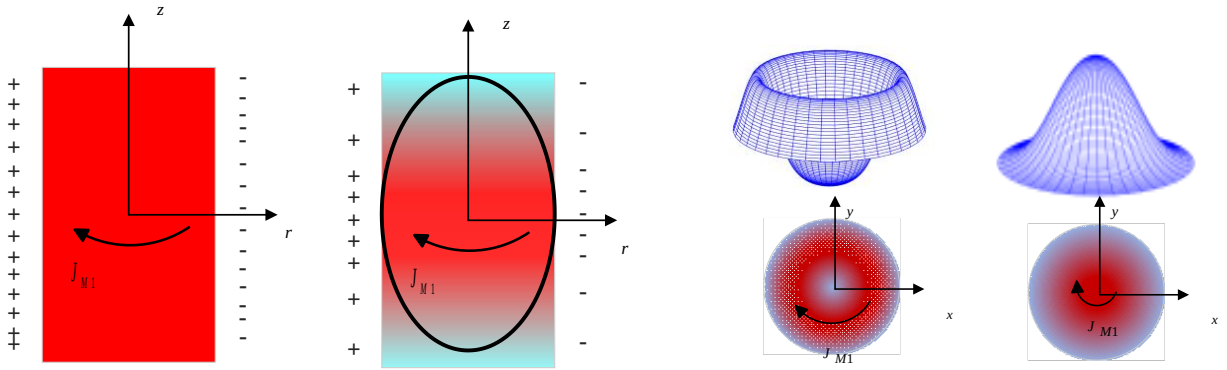

(a) Equivalent surface current axial distribution (b) Equivalent surface current radial distribution

Fig.5 Equivalent surface current axial distribution

Figure 5 shows that when the boundary surface of the magnetizing intensity distribution region is ellipsoidal, the equivalent current magnitude decreases from the middle section of the permanent magnet along the axis toward the ends. In the horizontal direction, the location of the magnetic flux density maximum shrinks from a ring towards the central axis as the radius of the cross-section decreases, forming a clear magnetic potential well structure.

Finally, the magnet array parameters are identified by PSO based on the above-modified model of magnet array parameters.

Table 1 PM array parameters

Symbol	Quantity	Values
a_1	Ellipse 1 long axis radius	3.6 mm
a_2	Ellipse 2 long axis radius	2.9 mm
b_1	Ellipse 1 short axis radius	0.8 mm
b_2	Ellipse 2 short axis radius	1.2 mm
Ms_1	Magnetization for inner cylinder magnet	7.82×10^5 A/m
Ms_2	Magnetization for outer ring magnet	9.21×10^5 A/m

Table 1 lists the parameters for the magnets array. Based on the identified permanent magnet parameters, the magnetic flux density along the radial direction of the permanent magnet array at suspension heights h=1.2 mm、h=1.7 mm、h=2.2 mm was calculated and compared with the experimental data, as shown in Figure 6.

The potential trap structure can generate diamagnetic force against the levitated rotor pointing toward a stable levitated position.

$$\boldsymbol{F} = \frac{x_m}{2u_0} \oiint_s B^2 \cdot \vec{n}_s dS \tag{6}$$

where x_m is the magnetic susceptibility, and x_m=-450×10^{-6}. From (6), it follows that the diamagnetic force on the levitated rotor at small displacements is proportional to the gradient of the magnetic potential energy, with the direction pointing from the high potential energy to the low potential energy.

The magnetic flux density was calculated based on the PM array parameters. On a horizontal surface with a levitation height h = 0.5 to 0.9 mm, the magnetic flux density is distributed along the radial direction, as shown in Figure 7. At a levitation height of 0.7 mm, the magnetic flux density decays along the axial direction, creating a diamagnetic force on

the pyrolytic graphite sheet along the axis, counteracting the effect of gravity, and achieving stable suspension in the axial direction. At a radial distance of 5 mm, the magnetic flux density increases along the radial direction, generating a diamagnetic force on the pyrolytic graphite sheet pointing towards the central axis and achieving a stable radial levitation of the pyrolytic graphite disc. According to (6), the distribution of diamagnetic force is calculated, as shown in Figure 8,

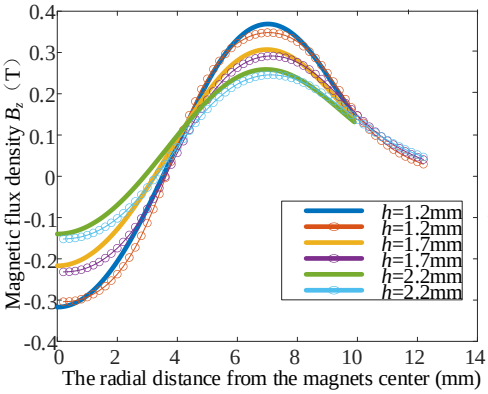

Fig.6 Axial magnetic flux density distribution

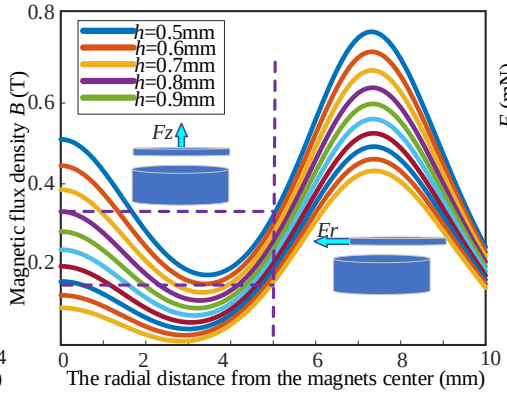

Fig.7 Magnetic flux density radial distribution

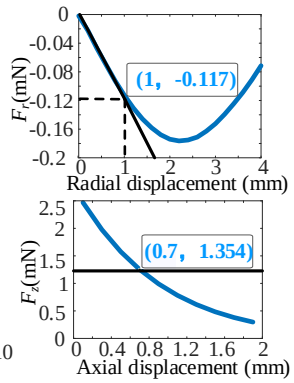

Fig.8 Diamagnetic force

The diamagnetic force on the levitated rotor increases along the radial direction from 0 to 2.5 mm radial displacement, with a maximum radial diamagnetic force of 1.8 mN. And the radial stiffness is equal to almost 0.14 N/m along the radial direction from 0 to 0.2 mm radial displacement.The diamagnetic force on the levitated rotor decreases along the axial direction. At a levitation height of 0.7 mm, the axial diamagnetic force on the pyrolytic graphite sheet is equal to 1.354 mN, counteracting the effect of gravity and achieving stable suspension in the axial direction. And the axial stiffness, greater than radial stiffness, equals almost 1.302 N/m.

3.2 Electronic Damping

The levitated rotor operates under the influence of air damping and electromagnetic damping[6]. At a levitation height of 0.7 mm, electromagnetic damping is the primary source of damping forces on levitation rotors. Pyrolytic graphite moving in a magnetic field generates eddy currents due to electromagnetic induction and is subject to a Lorentz force impeding the motion, which is expressed as follows

$$\boldsymbol{F} = \iint_{S_e} \boldsymbol{I} \times \boldsymbol{B} ds_e \tag{7}$$

When the levitated rotor is vibrating radially in the horizontal direction, as shown in Figure 9, the resulting induced current can be expressed as follows,

$$I_{r'} = -\frac{\partial D'}{r'\partial\theta'} \tag{8}$$

$$I_{\theta'} = -\frac{\partial D'}{\partial r'} \tag{9}$$

$$D = \frac{h}{4\pi\sigma}\oint_{S'} v_r \frac{\partial B_z}{\partial r}(r,\theta)\sqrt{\frac{R^4 + r_Q{}^2 r'^2 - 2r_Q r' R^2\cos(\theta_Q - \theta')}{R^2(r_Q{}^2 + r'^2 - 2r_Q r'\cos(\theta_Q - \theta'))}}\, dS_Q \tag{10}$$

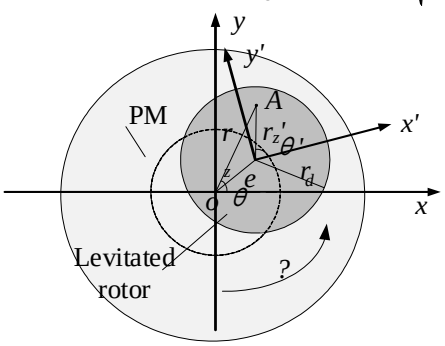

Fig. 9 vibration in the horizontal direction

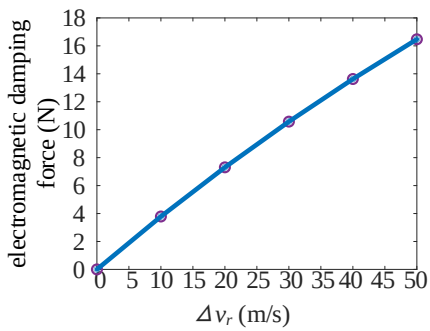

Fig. 10 electromagnetic damping force distrubution

The electromagnetic damping force of the pyrolytic graphite sheet at a distance of 0.2 mm from the center axis of the permanent magnet was calculated using Maxwell simulation and is shown in Figure 10, giving an electromagnetic damping of 3×10^{-4} N·s/m.

3.3 Dynamics Equation

From section 3.1, the rotor is subjected to diamagnetic forces from the permanent magnet stator in all five degrees of freedom, including the *z*-direction, *x* and *y*-directions. In addition, pyrolytic graphite has excellent electrical conductivity and generates eddy currents as well as electromagnetic damping when moving relative to the stator. The kinetic equations can be expressed as follows,

Due to the low speed of the diamagnetic levitated electrostatic motor and the weak influence of the gyroscopic effect on the rotor at low speeds, the rotor's inclination vibration is ignored. The kinetic equations for the rotor can be expressed as follows

$$m\ddot{x} + c_{xe}\dot{x} + k_{\alpha x}x = me\omega^2 \cos\omega t \quad (11)$$

$$m\ddot{y} + c_{xe}\dot{y} + k_{\alpha x}y = me\omega^2 \sin\omega t \quad (12)$$

$$m\ddot{z} + c_{ze}\dot{z} + k_z z = F_z \quad (13)$$

4. Experiments and Results

4.1 Experiments

Experiments measuring the radial stiffness, damping, and vibration were conducted to verify the dynamics model as shown in Fig. 11, Fig. 12, and Fig. 13.

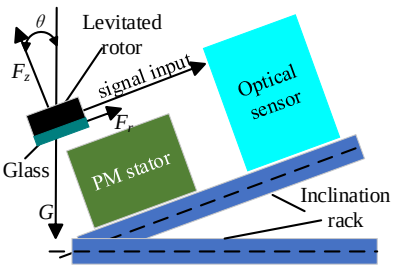

Fig.11 The radial diamagnetic force experiment

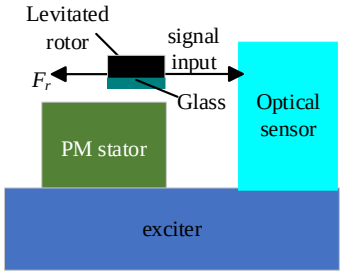

Fig.12 The electromagnetic damping experiment

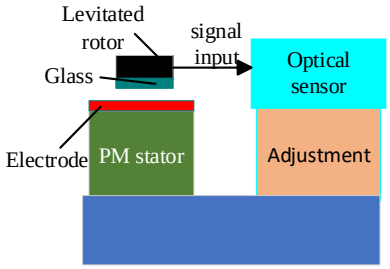

Fig.13 The radial vibration experiment

Fig. 11 shows the structure of the radial diamagnetic force experiment. From top to bottom are the levitated rotor (pyrolytic graphite + glass), the permanent magnets array, and the inclination rack. The inclination rack is used to tilt the permanent magnet. As the axial diamagnetic force cannot balance the gravity of the suspended rotor, the rotor will be displaced radially. Then the rotor is subjected to a certain radial diamagnetic force, which balances the gravity and allows the suspended rotor to return to a stable state of suspension.

Figure 12 shows the structure of the radial electromagnetic damping experiment. From top to bottom are the levitated rotor, the permanent magnets array, and the optical sensor, exciter. The exciter drives the PM array to vibrate horizontally, thereby displacing the levitated rotor relative to the PM array. The levitated rotor will vibrate around the stable suspended position with a gradual decay in amplitude.

Figure 13 shows the structure of. The levitated rotor (pyrolytic graphite + glass), the permanent magnets array, and the adjustment bracket are from top to bottom. The optical sensor is installed on a stand glued to the stator. The levitated rotor is suspended from the stator, with the glass side facing the stator. The laser emitted by the optical sensor illuminates the cylindrical surface of the levitated rotor by adjusting the position of the adjustment bracket.

4.2 Results

Results of the experiments measuring the radial stiffness, damping, and vibration is shown in Fig. 14, Fig. 15, and Fig. 16.

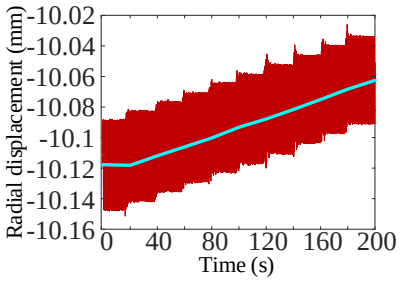

Fig.14 Radial displacement distribution

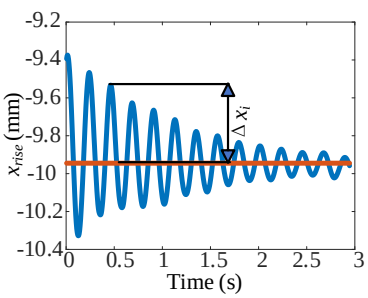

Fig.15 decay of the free response

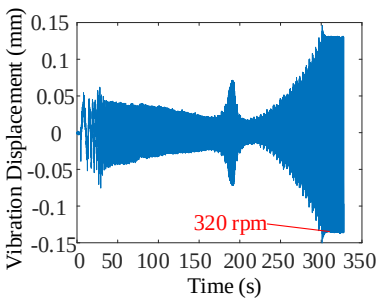

Fig.16 The vibration of the levitated rotor during acceleration

The radial diamagnetic force on the levitated rotor is quantitatively related to the degree of inclination, as shown in Figure 14.

$$F_r = mg\sin\theta = mg\frac{h_{rise}}{\sqrt{{h_{rise}}^2 + l^2}} \tag{14}$$

where l=600mm is horizontal distance between center of the hinge and the micrometer，h_{rise} is the height of the end of the plate being lifted. The radial diamagnetic force is proportional to the radial displacement of the levitated rotor between 0 and 0.06 mm, with a stiffness of approximately 0.135 N/m.

The decay of the radial free response amplitude of the levitated rotor under displacement excitation is shown in Fig. 15, which is related to the electronic damping,

$$\delta = \ln^{\frac{\Delta x_i}{\Delta x_{i+1}}} = \frac{2\pi\zeta}{\sqrt{1-\zeta^2}} \tag{15}$$

$$c = \zeta c_c = 2\sqrt{mk}\zeta \tag{16}$$

where δ is damping coefficient，Δx_i is the amplitude of the free response, ζ is the damping ratio, m=0.1354 g is the mass of the levitated rotor, k=0.135 N/m is the radial stiffness. The radial electromagnetic damping force is proportional to the radial vibration velocity, with average damping of approximately 3.05×10^{-4} N·s/m.

The change of the radial forced response of the levitated rotor with the frequency of input three-phase voltage increasing by 1 rpm at 1 s intervals is shown in Fig. 16. When the speed of the levitated rotor is increased to 300 rpm, the vibration is very intense, and the natural frequency could be calculated of 5.36 Hz. The calculated results are compared with the curve of the rotor vibration amplitude change in the experiment. The eccentricity of the mass of the rotor was identified at 0.02 mm.

5. Conclusion

This paper first establishes the kinetic equations of a diamagnetic levitated electrostatic motor. A magnetic field correction method for permanent magnet arrays is proposed and established based on the equivalent current model. Based on the principle of diamagnetic levitation, the diamagnetic force on the rotor during radial vibration has been modeled. Based on the principle of electromagnetic induction, the electromagnetic damping force on the rotor during radial vibration has been modeled. Meanwhile, the corresponding experiments were designed to verify the properties of the forces on the rotor.

The present study shows that the magnetization of the permanent magnets array decreases along the cross section, which causes the external magnetic field to form a potential well structure. The levitated rotor is subjected to a diamagnetic force proportional to the displacement, equivalent to a stiffness of 0.14 N/m. The levitated rotor is also subjected to an electromagnetic damping force proportional to the speed of motion, equivalent to a damping of 3.1 N/m·s^{-1}. When the speed of the suspended rotor is increased to 300 rpm it is very close to the first order intrinsic frequency and the vibration is very intense, meanwhile the eccentricity of the mass is 0.02 mm. The natural frequency could be calculated of 5.36 Hz.

References

[1] Jianquan L (2020) Magnetic levitation and Earnshaw theorem. Physics Teaching 42(8): 5.
[2] Furlani EP (2001) Permanent Magnet and Electromechanical Devices. San Diego: Academic Press, pp.129-143.
[3] Yuanping X, et al., (2017) Realization of a diamagnetically levitating rotor driven by electrostatic field. IEEE-ASME Transactions on Mechatronics, 22(5): 2387-2391.
[4] Yuanping X, et al., (2020) Modeling and Validation of Diamagnetic Rotor Levitated by Permanent Magnetics. Chinese Journal of Mechanical Engineering.
[5] Yongzhou H (2013) Study of the inhomogeneity of the external magnetic field of permanent magnets. Chinese Journal of Physics (08): 145-151.
[6] Xianfeng C, et al., (2022) Diamagnetic Composites for High-Q Levitating Resonators. Advanced science 9(32).